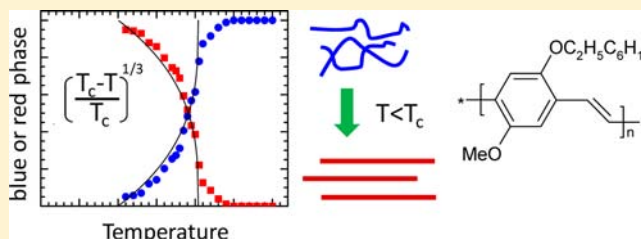


# An Order–Disorder Transition in the Conjugated Polymer MEH-PPV

Anna Köhler,\* Sebastian T. Hoffmann, and Heinz Bässler

Organic Semiconductors, Experimental Physics II, Department of Physics and Bayreuth Institute of Macromolecular Science (BIMF), University of Bayreuth, Bayreuth 95440, Germany

**ABSTRACT:** The poly(*p*-phenylene vinylene) derivative MEH-PPV is known to exist as two morphologically distinct species, referred to as red phase and blue phase. We show here that the transition from the blue phase to the red phase is a critical phenomenon that can be quantitatively described as a second order phase transition with a critical temperature  $T_c$  of 204 K. The criticality is associated with the trade-off between the gain in the electronic stabilization energy when the  $\pi$ -system of a planarized chain can delocalize and the concomitant loss of entropy. We studied this transition by measuring the absorption and fluorescence in methyltetrahydrofuran (MeTHF) in two different concentrations as a function of temperature. The spectra were analyzed based upon the Kuhn exciton model to extract effective conjugation lengths. At room temperature, the chains have effective conjugation lengths of about five repeat units in the ground state (the blue phase), consistent with a disordered defect cylinder conformation. Upon cooling below the critical temperature  $T_c$ , the red phase with increased effective conjugation lengths of about 10 repeat units forms, implying a more extended and better ordered conformation. Whereas aggregation is required for the creation of the red phase, its electronic states have a predominant intrachain character.



## 1. INTRODUCTION

Morphologically induced polychromism is a frequently encountered phenomenon in conjugated polymers. It was first recognized when studying the fluorescence from polydiacetylene in solution.<sup>1–4</sup> Depending on the kind of solvent, concentration and temperature, photoluminescence is emitted either from a high energy state (the “blue phase”) or from a lower energy state (the “red phase”) that differ in the extent of delocalization of the  $\pi$ -bond electrons.<sup>5</sup> There has been a lively debate whether or not this color change is a single chain phenomenon<sup>2,6</sup> or is rather a signature of aggregation.<sup>7,8</sup> While polychromism is of scientific interest as it indicates changes in the underlying electronic structure, it has also potential for commercial applications. For example, the temperature-dependence of absorption and emission in derivatives of polydiacetylene is being considered for sensor applications.<sup>9,10</sup>

A more recent, and for opto-electronic applications also more relevant example is the chromism that been observed in conjugated polymers of the poly(*p*-phenylene vinylene) family,<sup>11–21</sup> the poly(*p*-phenylene) family<sup>22–26</sup> and the polythiophene family.<sup>27–30</sup> In these materials, the polychromism indicates changes in electronic coupling between the molecular subunits. This has a strong impact on the performance of devices such as transistors, solar cells or light-emitting diodes.<sup>24,25,29–33</sup> Understanding the relationship between the conformation of polymer chains and their electronic structure in the excited state is thus a key issue in the field. We need to comprehend (i) which physical phenomenon causes the polychromism and its dependence on experimental parameters such as temperature, concentration

and molecular weight, and (ii) what is the role of intrachain and interchain interactions in this process.

In the current manuscript, we address the origin of the polychromism for the prototypical polymer MEH-PPV (poly-(2-methoxy-5-(2'-ethylhexyl)oxy 1,4-phenylene vinylene)). MEH-PPV is well-known to show a bimodal distribution of emission maxima.<sup>11–14,17,18,34–38</sup> The two associated chain conformations are referred to as “blue phase” and “red phase”. We measured the absorption and fluorescence spectra of MEH-PPV with molecular weight of about  $M_w = 60 \pm 10$  kD, equivalent to about  $230 \pm 40$  repeat units per chain, in methyltetrahydrofuran (MeTHF) solution between 300 K and 80 K. The concentrations were  $5 \times 10^{-6}$  mole of repeat unit/liter of solvent and  $10^{-7}$  mole of repeat unit/liter of solvent. The aim of this study is to gain insight into the condition and mechanism for the formation of a bimodal distribution of excited states in MEH-PPV.

Our results suggest that, (i) the transition from the blue phase to the red phase can be described as a cooperative phenomenon that leads to a second order (continuous) phase transition. It is associated with a disorder-to-order transition, corresponding to a change in the polymer structure. (ii) We find that both, intrachain and interchain interactions facilitate the establishment of the more ordered, that is, a red phase. Thus, in MEH-PPV the *formation* of the red phase is assisted by concentration dependent aggregation, yet the electronic *nature* of the excited state has a predominant intrachain character.

Received: March 12, 2012

Published: June 19, 2012

## 2. EXPERIMENTAL METHODS

MEH-PPV was purchased from American Dye Sources Ltd. (ADS), Canada, and dissolved in methyltetrahydrofuran (MeTHF) at a concentration of  $5 \times 10^{-6}$  mol/L and of  $1 \times 10^{-7}$  mol/L. The quantity “mol” refers to the repeat unit of the polymer. For the temperature-dependent measurements of absorption or fluorescence, the solution was filled in a fused silica cuvette and was placed in a continuous flow cryostat. The temperature was monitored using a home-built temperature controller. At each temperature, we waited for about 15 min to ensure a stable equilibrium temperature is obtained throughout the sample space. To acquire the absorption spectra, we excited using a tungsten lamp and recorded the transmission dispersed by a monochromator using a silicon diode and a lock-in amplifier. The spectra were corrected for the transmission of the setup. For the photoluminescence spectra, we excited at 405 nm (3.06 eV) using a diode laser and recorded the emission spectrum with a glass fiber connected to a spectrograph with a CCD camera attached (Oriol MS125 attached to Oriol Instaspect IV).

In order to separate the relative contribution from the blue phase and the red phase in absorption and emission, as well as in order to obtain more accurate energetic positions for the  $S_1-S_0$  0–0 transition and to derive the variance  $\sigma$  of the line width, we deconvoluted the absorption and emission bands using a Franck–Condon analysis as described in refs 22,39,40. For example, to model the absorption spectrum  $A(\hbar\omega)$  in photons/energy interval, we used the expression  $A(\hbar\omega) = n^{3*}(\omega)^3 \sum_{m_i} \Pi_i (e^{-S_i} S_i^{m_i}) / (m_i!) \Gamma \delta[\hbar\omega - (\hbar\omega_0 + \sum m_i \omega_i)]$ , where  $\hbar\omega_0$  is the energy of the 0–0 peak,  $\hbar\omega_i$  are the vibrational energies of the modes  $i$  taken from Raman spectra,  $m_i$  denotes the number of vibrational overtones,  $\Gamma$  is the Gaussian Lineshape operator, and  $S_i$  is the Huang–Rhys parameter for the mode  $i$ .  $\Gamma$  is related to the variance  $\sigma$  of the line width by  $\Gamma = (1/(2(2\pi)^{1/2})) e^{-((\hbar\omega - \hbar\omega_0)^2)/(2\sigma^2)}$ .  $n$  is the refractive index of the surrounding medium. For MeTHF, it is 1.4 and can be considered constant over the range investigated, since MeTHF is transparent in this spectral range. We considered two modes  $i$  and  $m_i = 4$  overtones for each mode. The modes considered were  $1306 \text{ cm}^{-1}$  (C=C stretching coupled to C–H bending of the vinyl group) and  $1586 \text{ cm}^{-1}$  (C–C stretching of the phenyl ring). These high-energy modes couple most strongly to the electronic excitations, as evident from their high Raman intensity. The numerous other active modes with low Raman intensity were not incorporated in this analysis. The two modes employed may thus be considered as effective modes. Importantly, the large number of low-energy modes such as torsions and librations are NOT included explicitly in  $A(\hbar\omega)$ . Instead, their contribution is, to some extent, subsumed in the variance  $\sigma$  of the line width.<sup>41</sup>

The temperature-dependent oscillator strength for the blue phase and the red phase was derived by considering by which factor  $F(T)$  the overall absorption increases with temperature relative to its value at the reference temperature  $T_0$  of 290 K, where all the absorption is due to the blue phase. If  $\phi_R$  and  $f_R(T)$  denote the compositional fraction of the red phase and its oscillator strength, and  $\phi_B$  and  $f_B(T)$  take the same meaning for the blue phase, it follows that  $\phi_R(T)f_R(T) + \phi_B(T)f_B(T) = F(T) * 1 * f_B(T_0 = 290)$ . From 300 to 220 K, less than 4% of absorption is due to the red phase (vide infra) and can be neglected. The increase in overall absorption (emission) intensity from 300 to 220 K translates in an increase in oscillator strength for the blue phase due to planarization by a factor of 1.1 (1.5). Below 210 K, where the red phase is formed, we have considered  $f_B$  to remain largely constant at 1.1 (1.5) times the 290 K value. With this,  $f_R(T)$  can be calculated.

## 3. RESULTS

Figure 1a–c shows the absorption and emission spectra taken from MEH-PPV in MeTHF solution within a temperature range of 300–80 K (300–110 K for emission) taken at a concentration of  $5 \times 10^{-6}$  mol/L. In Figure 1d, the luminescence at  $1 \times 10^{-7}$  mol/L is shown for comparison. The absorption spectra are a superposition of a broad, vibrationally unresolved band that shifts bathochromically

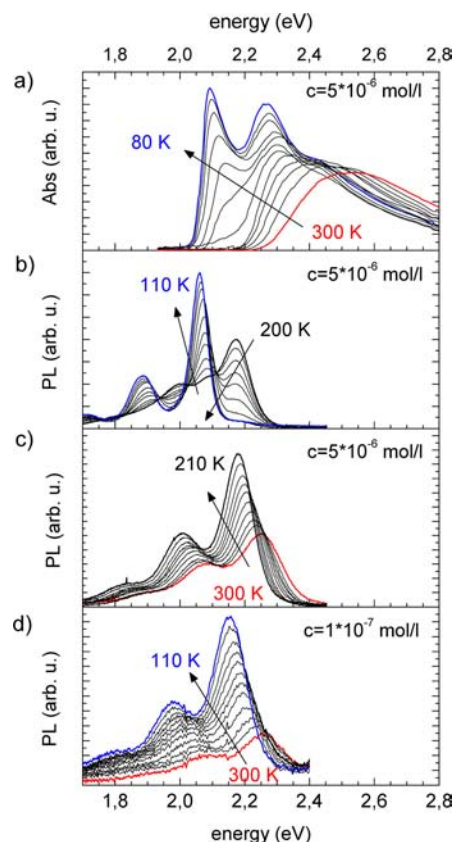


**Figure 1.** The optical transitions of MEH-PPV in MeTHF solution as a function of temperature, taken (a) for absorption in  $5 \times 10^{-6}$  M solution from 80 to 300 K in increments of 20 K, (b) for fluorescence in  $5 \times 10^{-6}$  M solution from 110 K to 200 K in increments of 10 K, (c) for fluorescence in  $5 \times 10^{-6}$  M solution from 210 to 300 K in increments of 10 K and (d) for fluorescence in  $10^{-7}$  M solution from 110 to 300 K in increments of 20 K.

from 2.50 to 2.25 eV upon cooling (the blue phase) and a vibrationally resolved spectrum with a  $S_1 \leftarrow S_0$  transition near 2.1 eV (the red phase) that grows upon cooling from 200 K onward.

Both phases fluoresce, and consequently, below 200 K, the fluorescence spectrum is supercomposed by emission from the blue phase with a 0–0 peak at about 2.20 eV and a red phase with a 0–0 peak at about 2.07 eV. Upon cooling, the intensity of the emission from the blue phase reduces while that of the red phase grows, giving rise to an isosbestic point. Obviously, there is a temperature induced transformation from the blue phase to the red phase. In the temperature range above 200 K, only fluorescence from the blue phase is observed. This emission shows a temperature-dependent shift of 0–0 energy and line width that is characteristic for disordered organics.<sup>39,42,43</sup> The mechanism for this temperature dependent energy shift will be analyzed in detail further below. Upon diluting the solution to a concentration of about  $10^{-7}$  mol/L, the emission of the red phase vanishes. For the entire temperature range from 300 to 110 K, the spectrum is that of the blue phase emission.

An emission or absorption band can be assigned to one or two emitting species when it can be modeled as either a single Franck–Condon progression or a superposition of two such progressions.<sup>22,40</sup> This is illustrated in Figure 2. At 290 K, absorption and emission can be modeled as a vibrational

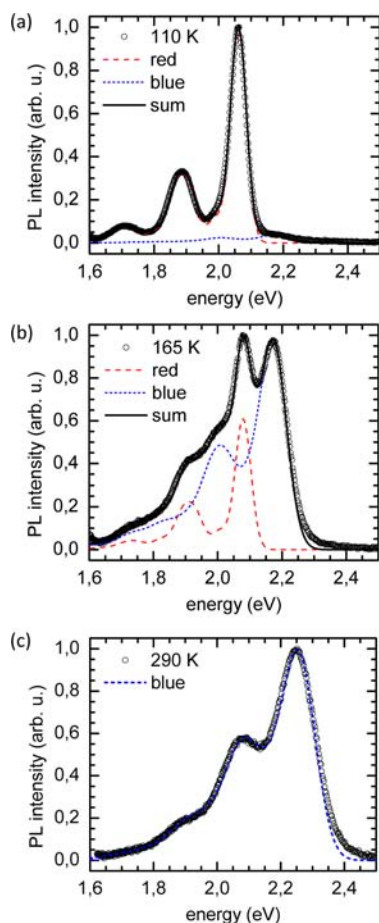


**Figure 2.** Franck–Condon fits to the fluorescence spectra of MEH-PPV taken in  $5 \times 10^{-6}$  M MeTHF solution (a) at 110 K, (b) at 165 K and (c) at 290 K. Shown are the fits to the blue phase (short dashes), to the red phase (dashes), the sum of both fits (solid line) and the experimental data (open circles).

progression of a single emitter. Our Franck–Condon fit uses a 0–0 energy at 2.260 eV and a disorder parameter  $\sigma = 51$  meV for the width of the Gaussian peaks used in the progression. In contrast, at 165 K, the spectra can only be reproduced by considering two progressions with 0–0 peaks located at 2.175 eV ( $\sigma = 40$  meV) and 2.079 eV ( $\sigma = 25$  meV) that have the same high-energy vibrational peaks, yet a different overall Huang–Rhys parameter and different line shape. As the temperature is reduced, the contribution from the higher energy, “blue” progression reduces until the spectrum is almost entirely dominated by the lower energy, “red”, progression at 110 K.

From the Franck–Condon analysis of the absorption and fluorescence spectra, we obtain the energies of the 0–0 transition as a function of temperature, shown in Figure 3a. By comparison with the 0–0 transition energies for entirely planar alkoxy-substituted phenylene vinylene oligomers (OPVs) we derive the effective conjugation length as follows. In recent work,<sup>39</sup> we have shown that in contrast to alkyl-substituted OPVs, alkoxy-substituted OPVs adopt fully planar structure. Their 0–0 energies can be fitted to the exciton model<sup>39,44</sup> that rests upon the particle in a box model developed by Kuhn and co-workers<sup>45,46</sup>

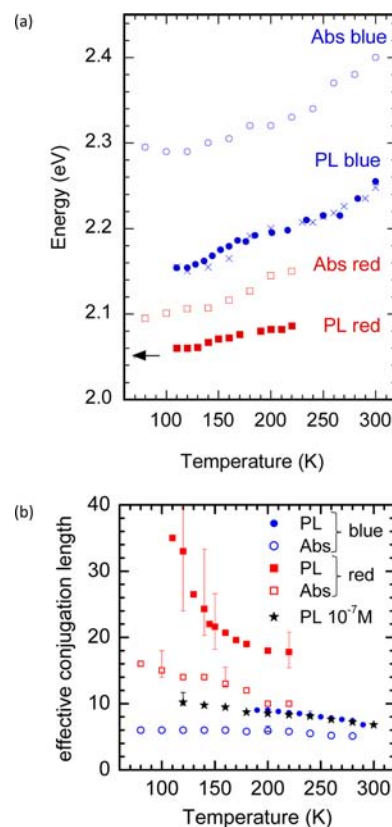


**Figure 3.** (a) The positions of the 0–0 peaks for absorption (open symbols) and emission (full symbols) obtained from the Franck–Condon fits, for the blue phase at  $5 \times 10^{-6}$  M (circles) and  $1 \times 10^{-7}$  M (crosses) solution, and for the red phase (squares) in  $5 \times 10^{-6}$  M solution. The arrow indicates the energy expected for emission from an infinitely long planar alkoxy-substituted PPV chain according to eq 1. (b) The effective conjugation length obtained by applying eq 1 to the values displayed in (a). A few exemplary error bars are indicated to illustrate the error obtained by eq 1 when the energy of the 0–0 position has an uncertainty of  $\pm 10$  meV.

$$E(N) = E_0 + 2\beta \cos\left(\frac{\pi}{N+1}\right) \quad (1)$$

with the parameters  $E_0 = 4.65$  eV,  $\beta = -1.30$  eV, and  $N$  being the number of repeat units. If we consider the 0–0 energy for the MEH-PPV chain and evaluate to which planar oligomer energy this corresponds, we derive the temperature dependent, mean effective conjugation length of for the blue phase that is displayed in Figure 3b. At room temperature, this turns out to be five repeat units in absorption and seven in emission. This value is in good agreement with the value of 7.6 repeat units found by De Leener et al. for the mean delocalization length for a 30-mer MEH-PPV oligomer on the basis of Monte Carlo simulations and quantum chemical calculations of the excited state in the isolated oligomer.<sup>47</sup> The Franck–Condon analysis of the fluorescence from the blue phase further yields a disorder parameter for the inhomogeneously broadened line shape of 51 meV. Part of this broadening results from fluctuations of the local polarization of the environment, yet some part represents a variation in conjugation length that, for the blue phase in MEH-PPV in solution, arises from torsions.<sup>39</sup> By comparison with our earlier work<sup>39</sup> we find the contribution of torsional induced disorder to the overall energetic disorder amounts to about 40 meV. This translates into a variance  $\sigma_N$  of  $\pm 0.5$  for the

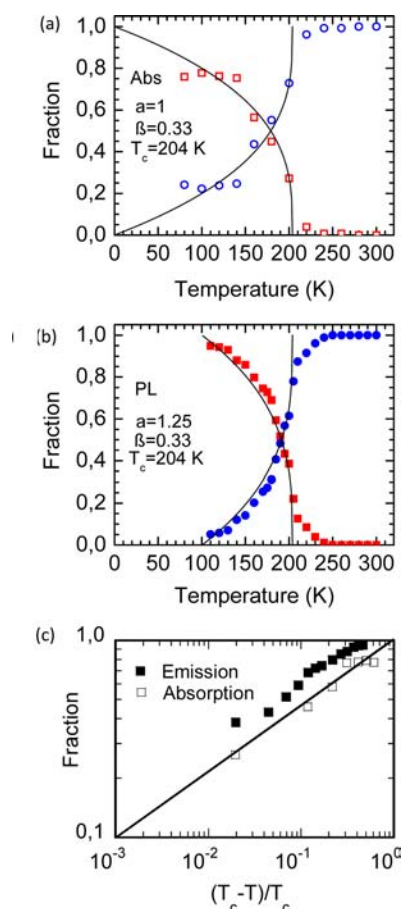
conjugation length of  $n_0 = 5$  repeat units, that is, roughly  $2/3$  of all chromophores in the blue phase have a conjugation length between 4.5 and 5.5 repeat units in absorption, reflecting the ground state geometry, and between 6.5 and 7.5 in emission. The longer conjugation length in emission represents the excited state geometry after relaxation and partly also after spectral diffusion to lower energy chromophores. The relative weight of the two factors and their dependence on temperature will be discussed in detail further below.

Figure 3b further shows that for the dilute sample at a concentration of  $10^{-7}$  mol/L, the effective conjugation length in the excited states increases continuously from 7 to 10 repeat units upon cooling from room temperature to 110 K. In the sample with  $5 \times 10^{-6}$  mol/L, the same conjugation lengths are obtained for the blue phase. There is an abrupt change, however, when the red phase is formed. In the red phase, the conjugation length in the excited state ranges from about 18 repeat units at 220 K to about 35 repeat units at 110 K. The values obtained at low temperature are subject to considerable error, since, based upon eq 1, the larger the effective conjugation length the smaller is the variation in the excited state energies.<sup>39</sup> We find the same trend for the ground state geometry, that is, a small increase in conjugation length from 5 to 6 repeat units upon cooling in the blue phase, yet a jump to 10 repeat units at 220 K when the red phase forms, increasing to 18 at 80 K. It is gratifying to note that the experimental value for the  $S_1 \rightarrow S_0$  0–0 transition of the red phase extrapolates to 2.05 eV. This is exactly the value predicted by eq 1 for an infinitely long chain using the parameters inferred from the PL spectra of the alkoxy-substituted phenylene vinylene oligomers.<sup>39</sup>

Using the deconvolution of the spectra, we can determine the fractional contribution of the blue and the red phase to the overall spectrum. To convert from the fraction of absorption by the red phase to the actual fraction of composition by the red phase, we need to correct for the increased oscillator strength in the red phase compared to the blue phase as detailed in the Experimental section above. It turns out that the increased conjugation length in the red phase leads to an oscillator strength that is about 1.5 times that of the blue phase at room temperature. Taking this into account, we obtain the fraction of red and blue phase in the overall composition presented in Figure 4. From room temperature to about 200 K, emission and absorption only involve the blue phase. From 200 K on, the red phase gains intensity. The key feature to notice is that the temperature-driven transformation from the blue to the red phase does not commence gradually. Instead, the phase transformation starts with a high rate of change near 200 K that only reduces at lower temperatures. Above 200 K, only a weak pretransitional red phase absorption/emission is observed. Empirically, we can functionalize the temperature dependences of the fraction  $f_R(T)$  of red phase and of the blue phase  $f_B(T)$  as

$$f_R(T) = a \left( \frac{T_c - T}{T_c} \right)^\beta \text{ and } f_B(T) = 1 - f_R(T) \quad (2)$$

A fit using the parameters  $T_c = 204$  K and  $\beta = 0.33$  is indicated in the figure, with  $a = 1$  for absorption and  $a = 1.25$  for emission. Such a temperature dependence is indicative of a second order phase transition. To allow for a better assessment of the quality of fit, the data is displayed in Figure 1c on a double logarithmic scale, with  $(204 - T)/204$  being the ordinate.



**Figure 4.** The fraction of red phase (squares) and blue phase (circles) in the overall composition as a function of temperature, (a) derived from the absorption spectra, (b) derived from the photoluminescence spectra. The solid line indicates a fit to eq 2, with the parameters as indicated in the figure. (c) The fraction of red phase derived from absorption (open symbols) and emission (full symbols) spectra, plotted on a double logarithmic normalized temperature difference scale, that is, against  $(T_c - T)/T_c$  for  $T_c = 204$  K. The solid line indicates a slope of  $1/3$ .

A slope of  $1/3$  is indicated as solid line. An overall good quality of fit is evident for the data resulting from the absorption spectra, with the fit predicting 100% red phase at 0 K. In the temperature range of about 110 K and below, the amount of red phase formed appears to saturate. We attribute this to the fact that while the melting point of MeTHF is usually listed as 80 K in common chemical data sheets, the viscosity of MeTHF increases from 110 to 80 K by more than 10 orders of magnitude, thus impeding further planarization of the chains.<sup>48</sup> When considering the compositional fraction of red phase observed in emission, we find the exactly same temperature dependence, yet the overall red phase fraction in emission is increased by about 25%, even at temperatures where the solvent becomes viscous. We take this to indicate some residual energy transfer from the blue to the red phase

#### 4. DISCUSSION AND CONCLUSIONS

The existence of a blue phase and a red phase is well documented for MEH-PPV.<sup>12–14,17,18,34–38</sup> There is, however, some discussion regarding the nature of the excited states involved.<sup>16,18,21,47</sup> There is widespread consensus that the blue phase is associated with an excitation of a single chromophore

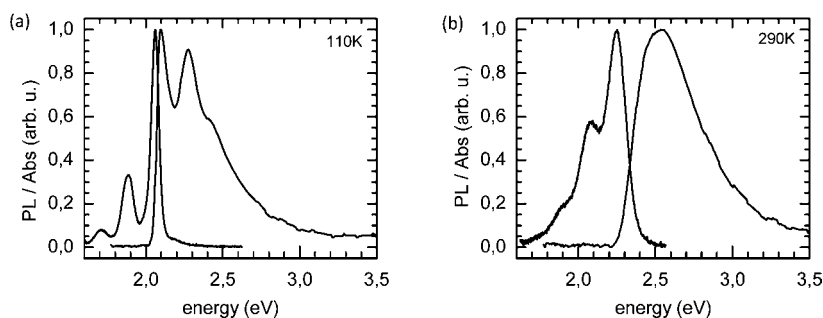


**Figure 5.** Comparison of the absorption and emission spectra obtained in  $5 \times 10^{-6}$  M MeTHF solution (a) at 110 K, where the red phase dominates, and (b) at 290 K, where the blue phase dominates.

on a MEH-PPV chain, i.e. a sequence of electronically coupled,  $\pi$ -conjugated repeat units along the chain that do not interact electronically with other chromophores. This blue phase prevails in dilute solution (Figure 1d). Its vibronic structure can be reproduced well by a Franck–Condon progression (Figure 2).<sup>39</sup> It is thus attributed to electronically isolated MEH-PPV chains.

In single molecule fluorescence measurements, where a blend of MEH-PPV and polycarbonate is spin-cast to form a thin film, a similar blue phase emission with a 0–0 peak at about 2.25 eV (550 nm) has been observed. By comparing the measured anisotropy of the polarized fluorescence with the anisotropy predicted from conformations simulated by Monte Carlo measurements, the emission from this blue phase has been associated with MEH-PPV chains that arrange in a more oblong, even compact, chain structure, referred to as “defect cylinder”.<sup>13,35,36,49</sup> Our solution spectra for the blue phase are very similar to the spectra of MEH-PPV/polycarbonate film, and the solvent we used, MeTHF, is known not to be a good solvent for MEH-PPV. We conjecture that the MEH-PPV chains in the solution in the blue phase therefore adopt a conformation similar to the “defect cylinder”, with rigid segments folded in a disordered way to a compact structure.

**4.1. Considering the Electronic Nature of the Two Phases.** The nature of the excitations that give rise to the red phase is more complex. We observe the red phase, with a 0–0 peak at 2.06 eV for PL at 110 K, in the more concentrated solutions (Figure 1). Its existence therefore benefits from some degree of aggregation.<sup>11,38,47</sup> Nevertheless, there is compelling evidence that absorption and emission in the red phase is not caused by interchain excitations such as excimers or H-aggregates. Excimers can be excluded as the red phase has its own absorption spectrum (Figure 1) and can be excited directly.<sup>18,21</sup> Transitions involving H-aggregates can be discarded since (i) the absorption and emission of the red phase shows a well resolved, narrow vibrational structure that can be fitted well by a single Franck–Condon progression (Figure 2), (ii) single molecule spectroscopy on MEH-PPV chains dispersed in PMMA matrix at 1.2 K show that the emission from selectively excited “blue” and “red” chromophores features sharp phonon lines, demonstrating clearly that both emissions originate from individual chromophores,<sup>18</sup> (iii) the energy difference between the blue phase and the red phase is on the order of less than 0.15 eV. This is significantly less than for example the  $\sim 0.7$  eV energy difference that exists between the disordered phase of poly(3-hexylthiophene) (P3HT) that consists of coiled chains and ordered phase of weakly interacting H-aggregates.<sup>27,29</sup> Electronic interactions leading to H-aggregates should result in a substantial energetic

stabilization of the excited state, and a shift of only 0.15 eV is at variance with this. (iv) Combined Monte Carlo/Quantum chemical calculation on the excited states of MEH-PPV-oligomers in the bulk indicate that  $\pi$  stacking does not lead to a spread of electronic excitations over neighbor chromophores.<sup>47</sup> Thus in summary, the red phase can be associated with excitations located predominantly on individual chromophores on MEH-PPV chains, even though it requires a sufficiently high local density of chains to form the red phase. This is evident from the disappearance of the red phase upon dilution in Figure 1, and it is consistent with the calculations by De Lener et al.<sup>47</sup> and fluorescence lifetime imaging microscopy measurements by Peteanu, Sherwood and coworkers.<sup>50,51</sup>

The red phase is at lower energy than the blue phase, implying a higher degree of conjugation. As this is not obtained by spreading significantly onto adjacent chains, it must be obtained by extension of the electronic  $\pi$ -coupling over a larger number of repeat units, suggesting a reduced torsional induced disorder. Like for the blue phase, we apply the exciton model (eq 1),<sup>39,44</sup> and we arrive at an average conjugation length of 10 (18) repeat units for the ground state (excited state) at 220 K, where the first chains in the red phase appear. This length increases with decreasing temperature to values around 15 (35) repeat units at 110 K, as already mentioned above. There is an increasing error associated with increasing conjugation length, since for long conjugation length, the changes in excited state energies are weak and even tend to zero for infinite conjugation ( $n \rightarrow \infty$  in eq 1), implying that the conjugation might be even larger. In any case, it is clear that in the red phase, the chain is significantly more elongated than in the blue phase. This results in a different electronic structure, as evident in Figure 5. Figure 5 shows the absorption and fluorescence spectra of the MEH-PPV chains in  $5 \times 10^{-6}$  M solution at 290 K, where only the blue phase prevails, and at 110 K, where the red phase dominates. In neither case do the spectra show a mirror symmetry. This is attributed in part to the fact that torsional relaxation prior to fluorescence can result in a narrower emission spectrum, and in part to the fact that emission may occur only from the longest and most ordered chains due to spectral diffusion to lower energy chromophores while absorption takes place into all chromophores.<sup>42,52</sup> This is well understood and leads to a more narrow emission spectra than absorption spectra. When this difference in disorder is taken into account, the absorption and emission spectra taken from the blue phase at 290 K are similar. In particular, their Huang–Rhys parameters are similar. In contrast to this, for the red phase the Huang–Rhys parameters for absorption and emission are obviously different. Such strong differences of the Huang–Rhys parameters are typically associated with intermolecular

coupling as is the case for weakly coupled J-aggregates.<sup>53–55</sup> Clearly, this phenomenon requires a detailed, quantitative analysis that is beyond the scope of the present paper. Here, we shall keep our focus on the temperature-driven transition between the blue and the red phase.

To summarize the insight gained so far, the bimodal distribution of transition energies with a blue phase and a red phase that is observed in our experiments and in experiments by others, can be attributed to a bimodal distribution of effective conjugation length.<sup>56–60,39</sup> At 220 K in the excited state, chromophores of the blue phase extend over about 9 units, while 18 units form a chromophore of the red phase. Thus, the two different emission energies correspond to two distinct phases of polymer.

**4.2. The Temperature Dependent Transformation between the Two Phases.** We now draw attention to the fact that the red phase does not evolve from the blue phase in a continuous manner. Upon lowering the temperature, one might naively expect the chromophores in the blue phase to planarize and the chains to elongate, until the chromophore length corresponding to the red phase is obtained. Figure 1 demonstrates that this is *not* the case. While the 0–0 energy of the blue phase shifts slightly with temperature, it does not move to the position of the 0–0 energy of the red phase. Rather, at a 200 K, the red phase transitions emerges at a spectrally distinct position from the blue phase transitions. For a few chains, the red phase is beginning to be formed at 220K, yet for most of the sample, red phase formation sets in at a critical temperature of 204 K. This pretransitional feature may be associated with either the longest and therefore less soluble chains in the molecular weight distribution or with critical fluctuations that are characteristic for a second order phase transition. When the fraction of absorption from the red phase and the blue phase are displayed as a function of temperature, a dependence is obtained that can be fitted with the eq 1, yielding a critical exponent of  $\beta = 0.33$ . The temperature driven transformation from the blue phase to the red phase can thus be described as a second order phase transition. The sudden appearance of long chromophores upon lowering the temperature is a cooperative phenomenon that is accompanied by a global change in structure and physical properties. It does not take place in the dilute,  $10^{-7}$  M solution.

What is causing this phase transition? The absence of red phase in the dilute solution implies that a certain minimum local concentration of chains is required. This fully agrees with the calculations and Monte Carlo simulations by De Leener et al.<sup>47</sup> They calculated and analyzed the conformation of MEH-PPV chains when they are isolated and when they are in a locally dense packing. For isolated chains, they find excitations to spread over chromophores of about eight repeat units. When the chains are packed more densely, they do not interact electronically, yet their conformational dynamics changes. These packing effects yield conjugated segments that have locally a more planar conformation. This is corroborated by NMR studies of Rothberg and co-workers who have shown that packing substantially reduces the flexibility of the backbone.<sup>11,21</sup> Consistent with this picture, Peteanu and co-workers report that oligomers of PPV form “core-shell” like structures in which the core consists of aggregated, that is, red emitting, chains, and the shell consists of monomer-like, that is, blue-emitting, chains that are indirect contact with the surrounding solvent.<sup>50,51</sup> Thus, from our experimental data (Figure 1), the microscopy work of Peteanu, the NMR data of Rothberg and the

calculations by De Leener it follows that one ingredient to this phase transition are intermolecular interactions such as e.g. van der Waals interactions leading to a locally dense packing which impacts on the chain conformation, reducing the possibility of torsional motion.

We note that the effect of dense packing is 2-fold. First, it restricts conformational dynamics. Second, it reduces contact with the MeTHF, which is a poor solvent for MEH-PPV.

We have already argued that the blue phase we observe in solution is similar to the defect cylinder morphology reported for single chains in a polycarbonate matrix. Obviously, this collapsed structure is largely driven by the fact that MEH-PPV and MeTHF do not mix well. The longer conjugation length found for the chromophores in the red phase implies that the red phase must be associated with a more extended, linear morphology, like a defect coil or toroid.<sup>13</sup> If the chain is to be more extended, yet solvent contact is still to be minimized, this can best be realized inside the bulk of a sufficiently large MEH-PPV phase, consistent with the observations by Peteanu and co-workers.

A second, related contribution to this phase transition is due to intramolecular interactions that stabilize a planar conformation. We had previously compared oligomers of the phenylene vinylene family carrying either an alkoxy- or an alkyl pendant group in MeTHF solutions.<sup>39</sup> We investigated the evolution of absorption and fluorescence spectra upon cooling. For the alkoxy derivatives, we find there is some chain aggregation that forces the chains into a highly ordered, planarized conformation below 180 K. In contrast for the alkyl derivatives, such a ordered state is not attained. Quantum chemical calculations of the ground and excited state geometry for a isolated trimer indicate that the equilibrium geometry in ground state is planar for the alkoxy derivative yet twisted for the alkyl derivative. This trend persists further in the excited state, albeit the difference between the two structures is less pronounced. It appears that the additional oxygen in the side group encourages a planar structure, maybe by electrostatic interactions between the oxygen in the side group and hydrogen on the main chain phenyl ring. From this we infer that the planar structure of the chromophores also requires an intramolecular driving force.

To get some insight into this phase transition it is instructive to consider the Gibbs free energy. For one phase, say the blue phase, this is given by  $G_{\text{blue}} = H_{\text{blue}} - TS_{\text{blue}}$  where  $G$  denotes the Gibbs free energy,  $H$  is the enthalpy,  $T$  the temperature and  $S$  the entropy. The Gibbs free energy for the red phase is analogous, and the difference between the Gibbs free energy of the two phases is given by  $\Delta G = \Delta H - T\Delta S$ . At a given temperature, the phase with the smaller  $G$  will form. Thus, at high temperature, the phase with the larger entropy prevails,<sup>61</sup> and this is evidently the disordered blue phase rather than the planar phase which is more restricted in its conformational possibilities. Upon cooling, however, a critical temperature is reached at 210 K when the gain in enthalpy,  $\Delta H$ , obtained by planarization, exceeds the entropic term  $T\Delta S$ . Formation of the red phase then becomes thermodynamically favored. Since the enthalpy depends on the extension of the  $\pi$ -electron system, this disorder-to-order transition is expected to be a cooperative phenomenon tractable in terms of the formalism of second order phase transitions.<sup>61</sup> This theory can also account for the pretransitional phenomenon near the critical temperature  $T_c$ . Regarding the entropic term, the role of torsional disorder is worth highlighting. In our work on the origin of the

inhomogeneously broadened line width in MEH-PPV,<sup>39</sup> we demonstrated that the torsional disorder of MEH-PPV in MeTHF solution follows roughly a  $T^{2/3}$  dependence, in agreement with predictions by Barford and co-workers.<sup>62,63</sup> In this way, the reduction of temperature leads by itself to a reduced conformational degree of freedom, i.e. entropy, that, at the critical temperature, can no longer compete with the gain in enthalpy upon planarization, in particular, as the torsional modes are strongly coupled to the electronic state of the polymer.<sup>41,52,64,65</sup>

In summary, we have demonstrated that the experimentally observed bimodal distribution of transition energies can be quantitatively described as a second order phase transition from a disordered, blue phase to a ordered, more planar red phase. A certain local density is required to allow for this phase transition. Further work should consider to which extend the critical temperature depends on molecular weight and polydispersity of the sample and on the quality of the solvent. With a view to other, related polymer structures, it would be interesting to consider by quantum chemical calculations the interplay between gain in  $\pi$ -electron energy upon planarization and possibly required geometric repulsion energy. This enthalpy term will need to balance any entropic term if such a phase transition is to also take place in other polymers.

## AUTHOR INFORMATION

### Corresponding Author

anna.koehler@uni-bayreuth.de

### Notes

The authors declare no competing financial interest.

## ACKNOWLEDGMENTS

Support from the doctoral training program GRK1640 of the Deutsche Forschungsgemeinschaft is acknowledged.

## REFERENCES

- (1) Chance, R. R.; Patel, G. N.; Witt, J. D. *J. Chem. Phys.* **1979**, *71*, 206.
- (2) Lim, K. C.; Sinclair, M.; Casalnuovo, S. A.; Fincher, C. R.; Wudl, F.; Heeger, A. J. *Mol. Cryst. Liq. Cryst.* **1984**, *105*, 329.
- (3) Patel, G. N.; Chance, R. R.; Witt, J. D. *J. Chem. Phys.* **1979**, *70*, 4387.
- (4) Rughooputh, S. D. D. V.; Bloor, D.; Phillips, D.; Jankowiak, R.; Schutz, L.; Bäessler, H. *Chem. Phys.* **1988**, *125*, 355.
- (5) Patel, G. N.; Witt, J. D.; Khanna, Y. P. **1980**, *18*, 1383.
- (6) Sinclair, M.; Lim, K. C.; Heeger, A. J. *Phys. Rev. Lett.* **1983**, *51*, 1768.
- (7) Wenz, G.; Müller, M. A.; Schmidt, M.; Wegner, G. *Macromolecules* **1984**, *17*, 837.
- (8) Müller, M. A.; Schmidt, M.; Wegner, G. *Makromol. Chem., Rapid Commun.* **1984**, *5*, 83.
- (9) Yarimaga, O.; Jaworski, J.; Yoon, B.; Kim, J. M. *Chem. Commun.* **2012**, *48*, 2469.
- (10) Kim, J. M.; Lee, Y. B.; Yang, D. H.; Lee, J. S.; Lee, G. S.; Ahn, D. *J. Am. Chem. Soc.* **2005**, *127*, 17580.
- (11) Collison, C. J.; Rothberg, L. J.; Treemanekarn, V.; Li, Y. *Macromolecules* **2001**, *34*, 2346.
- (12) Barbara, P. F.; Gesquiere, A. J.; Park, S. J.; Lee, Y. J. *Acc. Chem. Res.* **2005**, *38*, 602.
- (13) Hu, D. H.; Yu, J.; Wong, K.; Bagchi, B.; Rossky, P. J.; Barbara, P. F. *Nature* **2000**, *405*, 1030.
- (14) Yu, Z. H.; Barbara, P. F. *J. Phys. Chem. B* **2004**, *108*, 11321.
- (15) Kim, D. Y.; Grey, J. K.; Barbara, P. F. *Synth. Met.* **2006**, *156*, 336.
- (16) Mirzov, O.; Scheblykin, I. G. *Phys. Chem. Chem. Phys.* **2006**, *8*, 5569.
- (17) Feist, F. A.; Basche, T. *J. Phys. Chem. B* **2008**, *112*, 9700.
- (18) Feist, F. A.; Zickler, M. F.; Basche, T. *Chemphyschem* **2011**, *12*, 1499.
- (19) Feist, F. A.; Basche, T. *Angew. Chem., Int. Ed.* **2011**, *50*, 5256.
- (20) Pichler, K.; Halliday, D. A.; Bradley, D. D. C.; Burn, P. L.; Friend, R. H.; Holmes, A. B. *J. Phys.: Condens. Matter* **1993**, *5*, 7155.
- (21) Rothberg, L. In *Semiconducting Polymers*; Hadziioannou, G., Malliaras, G. G., Eds.; Wiley-VCH: Weinheim, 2007; Vol. 1, p 179.
- (22) Khan, A. L. T.; Sreearunothai, P.; Herz, L. M.; Banach, M. J.; Köhler, A. *Phys. Rev. B* **2004**, *69*, 085201.
- (23) Hayer, A.; Khan, A. L. T.; Friend, R. H.; Köhler, A. *Phys. Rev. B* **2005**, *71*, 241302(R).
- (24) Grell, M.; Knoll, W.; Lupo, D.; Meisel, A.; Miteva, T.; Neher, D.; Nothofer, H. G.; Scherf, U.; Yasuda, A. *Adv. Mater.* **1999**, *11*, 671.
- (25) Scherf, U.; List, E. J. W. *Adv. Mater.* **2002**, *14*, 477.
- (26) Peet, J.; Brocker, E.; Xu, Y. H.; Bazan, G. C. *Adv. Mater.* **2008**, *20*, 1882.
- (27) Clark, J.; Silva, C.; Friend, R. H.; Spano, F. C. *Phys. Rev. Lett.* **2007**, *98*, 206406.
- (28) Zen, A.; Pflaum, J.; Hirschmann, S.; Zhuang, W.; Jaiser, F.; Asawapirom, U.; Rabe, J. P.; Scherf, U.; Neher, D. *Adv. Funct. Mater.* **2004**, *14*, 757.
- (29) Scharsich, C.; Lohwasser, R. H.; Sommer, M.; Asawapirom, U.; Scherf, U.; Thelakkat, M.; Neher, D.; Köhler, A. *J. Polym. Sci., Part B: Polym. Phys.* **2012**, *50*, 442.
- (30) Chang, J. F.; Sun, B. Q.; Breiby, D. W.; Nielsen, M. M.; Solling, T. I.; Giles, M.; McCulloch, I.; Sirringhaus, H. *Chem. Mater.* **2004**, *16*, 4772.
- (31) Herrmann, D.; Niesar, S.; Scharsich, C.; Köhler, A.; Stutzmann, M.; Riedle, E. *J. Am. Chem. Soc.* **2011**, *133*, 18220.
- (32) Turner, S. T.; Pingel, P.; Steyrlleuthner, R.; Crossland, E. J. W.; Ludwigs, S.; Neher, D. *Adv. Funct. Mater.* **2011**, *21*, 4640.
- (33) Lin, H. Z.; Tian, Y. X.; Zapadka, K.; Persson, G.; Thomsson, D.; Mirzov, O.; Larsson, P. O.; Widengren, J.; Scheblykin, I. G. *Nano Lett.* **2009**, *9*, 4456.
- (34) Grey, J. K.; Kim, D. Y.; Donley, C. L.; Miller, W. L.; Kim, J. S.; Silva, C.; Friend, R. H.; Barbara, P. F. *J. Phys. Chem. B* **2006**, *110*, 18898.
- (35) Ebihara, Y.; Habuchi, S.; Vacha, M. *Chem. Lett.* **2009**, *38*, 1094.
- (36) Ebihara, Y.; Vacha, M. *J. Phys. Chem. B* **2008**, *112*, 12575.
- (37) Nguyen, T. Q.; Wu, J. J.; Doan, V.; Schwartz, B. J.; Tolbert, S. H. *Science* **2000**, *288*, 652.
- (38) Nguyen, T. Q.; Doan, V.; Schwartz, B. J. *J. Chem. Phys.* **1999**, *110*, 4068.
- (39) Hoffmann, S. T.; Bäessler, H.; Köhler, A. *J. Phys. Chem. B* **2010**, *114*, 17037.
- (40) Ho, P. K. H.; Kim, J. S.; Tessler, N.; Friend, R. H. *J. Chem. Phys.* **2001**, *115*, 2709.
- (41) Karabunarliev, S.; Bittner, E. R.; Baumgarten, M. *J. Chem. Phys.* **2001**, *114*, 5863.
- (42) Hoffmann, S. T.; Bäessler, H.; Koenen, J. M.; Forster, M.; Scherf, U.; Scheler, E.; Strohriegel, P.; Köhler, A. *Phys. Rev. B* **2010**, *81*, 115103.
- (43) Meskers, S. C. J.; Hubner, J.; Oestreich, M.; Bäessler, H. *J. Phys. Chem. B* **2001**, *105*, 9139.
- (44) Chang, R.; Hsu, J. H.; Fann, W. S.; Liang, K. K.; Chiang, C. H.; Hayashi, M.; Yu, J.; Lin, S. H.; Chang, E. C.; Chuang, K. R.; Chen, S. A. *Chem. Phys. Lett.* **2000**, *317*, 142–152.
- (45) Kuhn, H. *Angew. Chem.* **1959**, *71*, 93.
- (46) Bär, F.; Huber, W.; Handschig, G.; Martin, H.; Kuhn, H. *J. Chem. Phys.* **1960**, *32*, 470.
- (47) De Leener, C.; Hennebicq, E.; Sancho-Garcia, J. C.; Beljonne, D. *J. Phys. Chem. B* **2009**, *113*, 1311.
- (48) Fischer, G.; Fischer, E. *Mol. Photochem.* **1977**, *8*, 279.
- (49) Hu, D. H.; Yu, J.; Padmanaban, G.; Ramakrishnan, S.; Barbara, P. F. *Nano Lett.* **2002**, *2*, 1121.
- (50) Peteanu, L. A.; Sherwood, G. A.; Werner, J. H.; Shreve, A. P.; Smith, T. M. *J. Phys. Chem. C* **2011**, *115*, 15607.

- (51) Sherwood, G. A.; Cheng, R.; Smith, R. M.; Werner, J. H.; Shreve, A. P.; Peteanu, L. A.; Wildeman, J. J. *Phys. Chem. C* **2009**, *113*, 18851.
- (52) Hwang, I.; Scholes, G. D. *Chem. Mater.* **2011**, *23*, 610.
- (53) Spano, F. C.; Yamagata, H. *J. Phys. Chem. B* **2011**, *115*, 5133.
- (54) Yamagata, H.; Spano, F. C. *J. Chem. Phys.* **2011**, 135.
- (55) Niles, E. T.; Roehling, J. D.; Yamagata, H.; Wise, A. J.; Spano, F. C.; Moule, A. J.; Grey, J. K. *J. Phys. Chem. Lett.* **2012**, *3*, 259.
- (56) Scholes, G. D.; Fleming, G. R. *J. Phys. Chem. B* **2000**, *104*, 1854.
- (57) Scholes, G. D. *Annu. Rev. Phys. Chem.* **2003**, *54*, 57.
- (58) Beenken, W. J. D.; Pullerits, T. *J. Phys. Chem. B* **2004**, *108*, 6164.
- (59) Narwark, O.; Gerhard, A.; Meskers, S. C. J.; Brocke, S.; Thorn-Csanyi, E.; Bäessler, H. *Chem. Phys.* **2003**, *294*, 1.
- (60) Narwark, O.; Gerhard, A.; Meskers, S. C. J.; Brocke, S.; Thorn-Csanyi, E.; Bäessler, H. *Chem. Phys.* **2003**, *294*, 17.
- (61) Jones, R. A. L. *Soft Condensed Matter*; Oxford University Press: Oxford, 2006.
- (62) Barford, W.; Trembath, D. *Phys. Rev. B* **2009**, *80*, 165418.
- (63) Makhov, V. D.; Barford, W. *Phys. Rev. B* **2010**, *81*, 165201.
- (64) Dykstra, T. E.; Hennebicq, E.; Beljonne, D.; Gierschner, J.; Claudio, G.; Bittner, E. R.; Knoester, J.; Scholes, G. D. *J. Phys. Chem. B* **2009**, *113*, 656.
- (65) Tretiak, S.; Saxena, A.; Martin, R. L.; Bishop, A. R. *Phys. Rev. Lett.* **2002**, *89*, 097402.